
EFDA–JET–CP(07)03/05

L. Carraro, C. Angioni, C. Giroud, M.E. Puiatti, M. Valisa, P. Buratti, R. Buttery,
I. Coffey, L. Garzotti, D. Van Eester, L. Lauro Taroni, K. Lawson, E. Lerche,
P. Mantica, M. Mattioli, V. Naulin and JET EFDA contributors

Impurity Profile Control in JET Plasmas with Radio-Frequency Power Injection

"This document is intended for publication in the open literature. It is made available on the understanding that it may not be further circulated and extracts or references may not be published prior to publication of the original when applicable, or without the consent of the Publications Officer, EFDA, Culham Science Centre, Abingdon, Oxon, OX14 3DB, UK."

"Enquiries about Copyright and reproduction should be addressed to the Publications Officer, EFDA, Culham Science Centre, Abingdon, Oxon, OX14 3DB, UK."

Impurity Profile Control in JET Plasmas with Radio-Frequency Power Injection

L. Carraro¹, C. Angioni², C. Giroud⁴, M.E. Puiatti¹, M. Valisa¹, P. Buratti³,
R. Buttery⁴, I. Coffey⁵, L. Garzotti⁴, D. Van Eester⁶, L. Lauro Taroni¹,
K. Lawson⁴, E. Lerche⁶, P. Mantica⁷, M. Mattioli¹, V. Naulin⁸
and JET EFDA contributors*

¹*Consorzio RFX – Associazione EURATOM-ENEA sulla Fusione, Padova, Italy*

²*Max Planck Institut für Plasmaphysik, EURATOM-IPP Association, D-85748 Garching, Germany*

³*EURATOM-ENEA Association, C.R. Frascati, CP 65, 00044 Frascati, Italy*

⁴*EURATOM/UKAEA Fusion Association, Culham Science Centre, Abingdon, OX14 3DB, UK*

⁵*Department of Physics, Queen's University, Belfast, United Kingdom*

⁶*Association EURATOM-Belgian State, LPP-ERM/KMS, Partner in TEC, B-1000 Brussels, Belgium*

⁷*IFP – Associazione EURATOM-ENEA sulla Fusione, Milano, Italy*

⁸*Association EURATOM-Risoe National Laboratory Technical University of Denmark*

* See annex of M.L. Watkins et al, "Overview of JET Results",
(Proc. 21st IAEA Fusion Energy Conference, Chengdu, China (2006)).

Preprint of Paper to be submitted for publication in Proceedings of the
34th EPS Conference on Plasma Physics,
(Warsaw, Poland 2nd - 6th July 2007)

1. INTRODUCTION

Various experiments have shown that injection of Radio-Frequency (RF) power may generate an outward pinch for impurities, with corresponding flattening of the impurity density profiles [1-7]. The effect has been found to be more pronounced when [2, 8] the power is applied to electrons rather than to ions and when it is centrally deposited. Therefore, the application of RF power may represent an active means to heal regimes that would otherwise be inclined to accumulate impurities.

This paper presents the results of Ni ($A = 28$), Mo ($A = 42$) Laser Blow Off (LBO) and Ar/Ne puffing experiments, in JET discharges featuring the injection of RF power at ITER relevant collisionality ($\nu_{\text{eff}} < 0.2$), aiming at studying the effect of different power levels when Ion Cyclotron Resonance Frequency (ICRF) is applied to electrons either as H Minority Heating (MH), or as Mode Conversion (MC) on 15-18% concentration of ^3He . Spectroscopic and Soft X-Ray data have been reconstructed by a 1D Collisional-Radiative (CR) impurity transport code, to evaluate the diffusion coefficient D and the pinch velocity V .

2. IMPURITY TRANSPORT AND RF POWER

Six H-mode or Hybrid low collisionality discharges with low MHD activity and with LBO injections of Ni have been selected for the impurity transport analysis. For these discharges, $\nu_{\text{eff}} \leq 0.2$ ($\nu_{\text{eff}} = 10^{-14} \langle n_e \rangle \langle T_e \rangle^{-2} Z_{\text{eff}} R$, with n_e in m^{-3} , T_e in eV, R the major radius in m, the symbol $\langle \rangle$ denotes a volume average), the elongation is about 1.7, lower triangularity is 0.18, higher triangularity 0.15. In addition, results regarding one Mo LBO injection and the CX data analysis of Ar/Ne puffings will be also discussed. In Fig.1 electron density, electron and ion temperatures and safety factor profiles at the time of LBO are shown for two of the six discharges.

The reference discharge (Pulse No: 69808) is without RF power. In the others, different values of ICRF power are delivered to electrons: 2MW in ^3He MC in Pulse No's: 66432 and 66434, 5.1MW in ^3He MC for Pulse No: 58149 and the very similar Pulse No: 58143, 8.3MW in H MH for Pulse No: 68383. The ICRF power deposition profiles are localized near the plasma centre, at about $\rho = 0.1$. In Fig.2 the power deposition profiles for ions and electrons are shown for the reference discharge (Pulse No: 69808) and for the discharge with the maximum ICRF power (Pulse No: 68383).

In order to evaluate the best estimate of the impurity (Ni) diffusion coefficient D and of the pinch velocity V , the experimental SXR brightness profiles, time behaviour and the time evolution of selected spectral lines during the LBO pulse have been reproduced with a 1-dim CR model [9,10] coupled to a mean square deviation procedure, minimizing the difference between simulated and experimental signals (minimizing χ^2). The time behavior of the Ni XVIII 292 Å line, pertaining to the plasma edge, is tracked to estimate the edge D and V and the Ni influx.

The solutions D and V of the least squares procedure are looked for into a restricted class of simple functions, linear between two consecutive spatial points (knots); the minimization procedure is repeated with different locations of the knots. The obtained D , V , and $-V/D$ for Pulse No's: 69808

and 68383 discharges are drawn in Fig.3: the stripes on D and V represent the uncertainties and are the set of results of the minimization procedure, with the different choice of the spatial knots. These uncertainties are greater than those evaluated from the matrix of covariance errors [11] for the single choice of knots.

The stripes on the peaking factors are obtained at each radial position as all the possible values of the ratio between -V and D.

Considering the SXR channels with LOS impact parameters $P < 0.5$ and SXR experimental uncertainties of 10%, best reproductions of experimental data give $\chi^2 = 3$ (Pulse No: 68383) and $\chi^2 = 4.5$ (Pulse No: 69808).

The pinch velocity of Fig.3 becomes outward in the discharge with high RF power, which features a higher diffusion too. The Ni peaking factors and their uncertainties derived in the six discharges at $\rho = 0.2$ and in a more external region at $r=0.5$, are shown in Fig.4 versus the ICRF power. It is worth to be noted (see Fig.4) that the same peaking factors as for Ni have been derived for the heavier species Mo ($A=42$), injected in the hybrid Pulse No: 68381 (very similar to the Pulse No: 68383 with Ni).

In the plasma centre the peaking factor becomes negative (corresponding to an outward pinch) for ICRF powers ≥ 5 MW. With already an ICRF power of 2 MW a peaking factor close to zero is found. However, due to the wide error bars, only a more statistically relevant database would allow the identification of a power threshold for the convection inversion.

At $\rho = 0.5$, as shown in Fig.3, the pinch velocity is inward w/o RF and outward for the higher value of ICRF, the peaking factors for the various RF powers remain close to zero, due to the higher values of the diffusion coefficients.

The transport analysis for impurities of different mass (C, Ne, Ar) has also been done in two additional Hybrid discharges [12], one without RF and the other with 3.3 MW of ICRF power (MH on H), where, besides Ni LBO, Ne and Ar were puffed into the plasma. The results, obtained by the transport code SANCO+UTC [13], confirm the inversion of the pinch from negative to positive, for those impurities as well (Fig.5). The peaking factors of Fig.4 and Fig.5 should not be quantitatively compared, since in the shots relative to Fig.5 a strong MDH $n = 1$ activity has been observed, whose effects have still to be examined.

3. RF POWER AND METAL POLLUTION

The Ni density profiles at the steady state have been calculated by extrapolating the simulation corresponding to the minimum value of χ^2 , with a constant Ni influx. In Fig.6 the normalized Ni total density profiles, for the discharge W/O RF (Pulse No: 69808) and for the discharge with the maximum ICRF power (Pulse No: 68383) are shown and compared with the electron density profiles. A favorable Ni hollow profile is found for the high ICRF power case. As a counterpart, it has to be pointed out that the measured Z_{eff} in the high ICRF discharge Pulse No: 68383 increases during the ICRF phase from 2 to 4–5 and that the enhancement is ascribed to metals (Z_{eff} from carbon charge

exchange data does not increase). Similar findings are reported in the literature [14-17]: further studies are necessary to understand in which plasma conditions the impurity profile flattening effect of heating electrons is associated with a tolerable increase of Z_{eff} . This is of particular interest at JET also in view of the installation of the new ICRF antenna [18]. In AUG [14] ECRH has been found to be less perturbing the total impurity content, suggesting that it could be a better candidate for central heating.

4. GS2 SIMULATIONS.

Quasi linear gyrokinetic GS2 [19] simulations of the experiments show that both with and w/o RF (Pulse No's: 68383 and 69808 respectively) the most unstable mode is ITG, with an associated inward pinch [20]. However, for the Pulse No: 68383 plasma parameters at $\rho = 0.35$, GS2 predicts a suppression of ITG instabilities if the ion temperature logarithmic gradient is $R/L_{Ti} \leq 3.5$. In such a case a TEM produces the Ni convection directed outwards, as shown in Fig.7. Lower values of R/L_n and of q in this case favor outward direction of the pinch.

In Pulse No: 68383 the experimental values of R/L_{Ti} are about twice the required for the transition to outward convection and the pinch velocity results to be outward all over the radius. Therefore Quasi Linear simulations do not match the experiment. To clarify if the superposition of the dominant ITG microinstability and the sub-dominant TEM is consistent with the experimentally found outward pinch, non linear calculations are needed.

CONCLUSIONS

The effect on Ni transport of different power amplitudes of ICRF applied to electrons has been explored in JET H-mode and Hybrid discharges. In the central plasma, hollow impurity profiles are found in discharges with strong centrally deposited ICRF applied to electrons (~8-9MW), corresponding to a pinch velocity outward directed. About 2 MW of RF injection results in flat Ni profiles; peaked profiles corresponding to an inward pinch are found when no RF is applied. A peaking factor very similar to that found for Ni has been evaluated for Mo at the higher values of ICRF. Due to the high mass of Mo, this result is important in the view of using W as plasma facing material. Small peaking factors are found in the more external region $\rho = 0.5$, due to the higher values of the diffusion coefficient. Discharges with high ICRF powers are found to be affected by metal contamination and the enhancement of the plasma effective charge counteracts the positive effect of reducing the central impurity peaking: therefore the identification of the ICRF power level and plasma conditions where the favourable impurity profile flattening effect is associated with a tolerable increase of Z_{eff} becomes an important issue.

ACKNOWLEDGEMENTS

This work, carried out under the European Fusion Development Agreement, supported by the European Communities has been carried out within the Contract of Association between EURATOM.

The views and opinions expressed herein do not necessarily reflect those of the European Commission

REFERENCES

- [1]. R. Neu et al Plasma Phys. Control. Fusion **44**, 811 (2002)
- [2]. R. Dux et al. Plasma Phys. Control. Fusion **45**, 1815 (2003)
- [3]. P. Gohil et al Plasma Phys. Control. Fusion **45**, 601, (2003)
- [4]. H. Takenaga et al Nucl Fusion **43**, 1235 (2003)
- [5]. E.S. Marmor et al. Nucl Fusion **43**, 1610 (2003)
- [6]. M.E. Puiatti et al Plasma Phys. Control. Fusion **45** (2003) 2011
- [7]. E. Scavino et al Plasma Phys. Control. Fusion **46** (1004) 857
- [8]. M.E. Puiatti et al Phys. Plasmas **13**, 042501 (2006)
- [9]. M. Mattioli et al. J.Phys. B34, **127** (2001)
- [10]. M. Mattioli et al. J.Phys. B37, **13** (2004)
- [11]. A.D. Whiteford PHD thesis, Strathclyde University, Glasgow (2004)
- [12]. C. Giroud et al. P2.049 This conference
- [13]. C. Giroud et al. Nucl. Fusion **47** (2007) 313
- [14]. R. Neu et al J. Nucl. Mater. **363-365** (2007) 52
- [15]. R. Dux et al J. Nucl. Mater. **363-365** (2007) 112
- [16]. S.J. Wukitch et al al J. Nucl. Mater. **363-365** (2007) 491
- [17]. M. Bures et al Plasma Phys. Control. Fusion **33**, (1991),93
- [18]. F. Durodié, et al , Fusion Engineering and Design **74** (2005) 223-228
- [19]. M. Kotschenreuther, G. Rewoldt, W.M. Tang, Comput. Phys. Commun. **88**, 128 (1995)
- [20]. C. Angioni et al. Phys. Plasmas **14**, 055905 (2007).

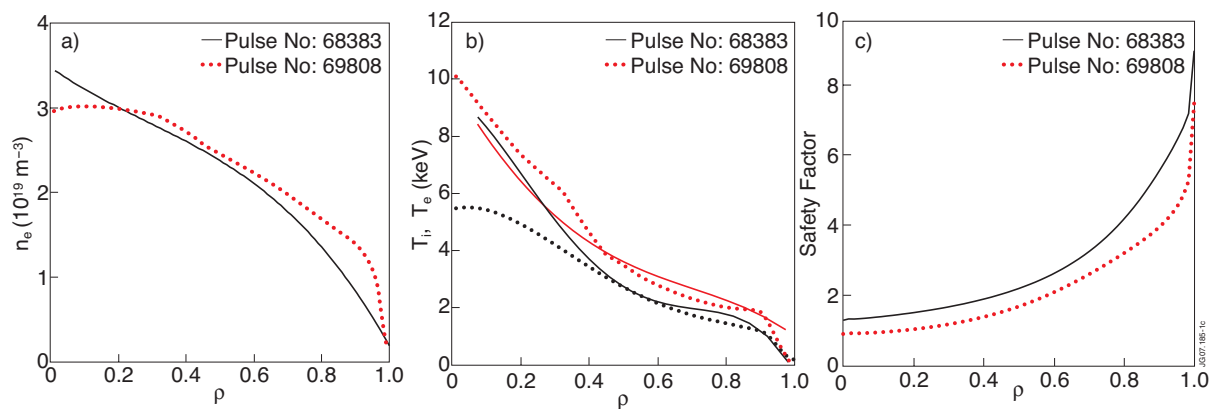


Figure 1: (a) Electron density profiles from interferometer data, b) Electron (dashed lines) and ion (solid lines) temperatures c) Safety factor profiles. All at the time of Ni LBO times, for the reference shot w/o RF (Pulse No: 69808) and for the shot with the higher ICRF power (Pulse No: 68383)

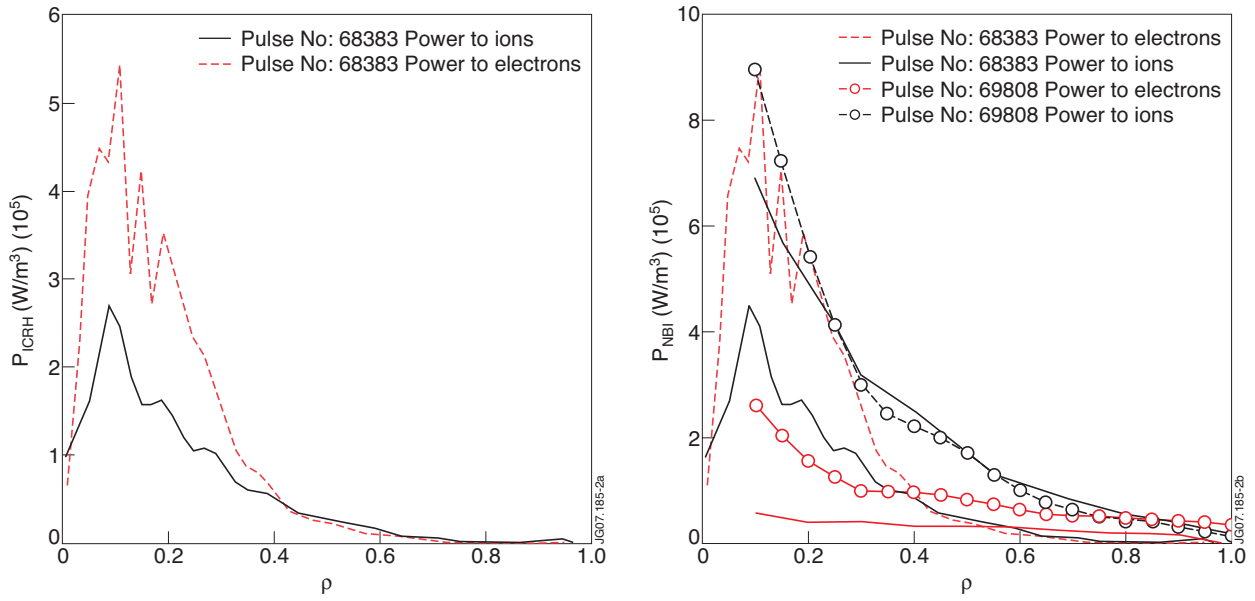


Figure 2: (a) ICRF and (b) NBI Electron and ion power deposition profiles for the reference discharge w/o RF Pulse No: 69808 and for the discharge with the maximum ICRF power Pulse No: 68383.

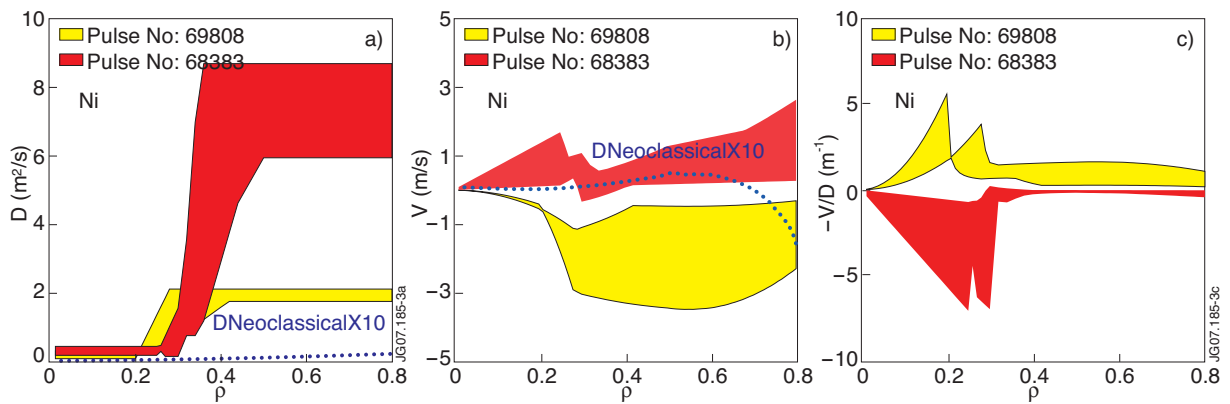


Figure 3: Ni Diffusion coefficient (left), pinch velocity (centre) and peaking factor ($-V/D$ right) for Pulse No's: 69808 and 68383.

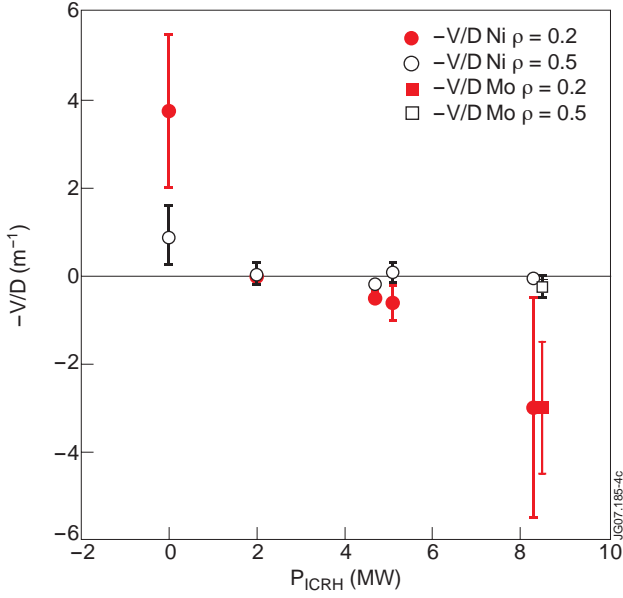


Figure 4: Ni peaking factors at $\rho=0.2$ and $\rho=0.5$ versus ICRF powers for the 6 discharges, Mo peaking factors for Pulse No: 68381.

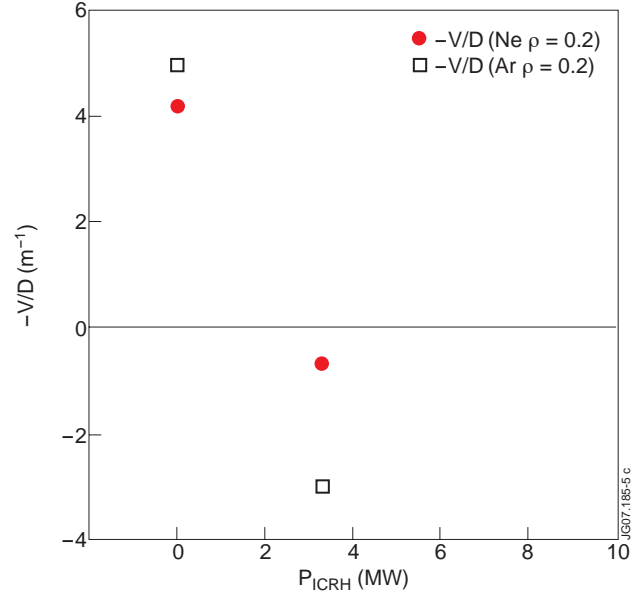


Figure 5: Ne and Ar peaking factors at $\rho=0.2$ w/o RF and with 3.3MW ICRF.

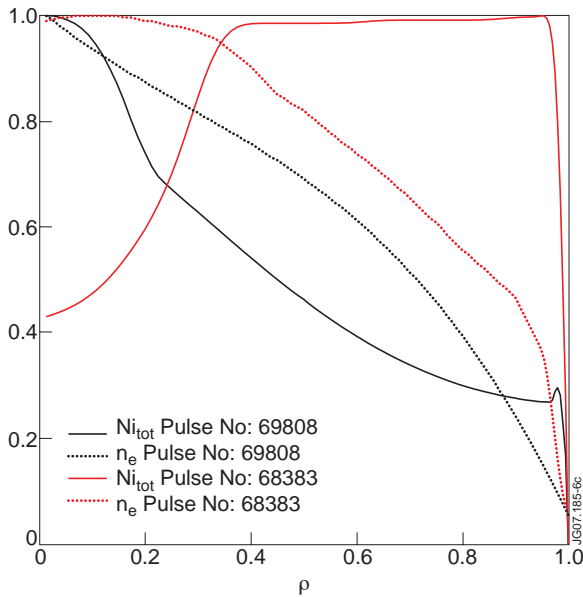


Figure 6: Stationary total Ni and electron density profiles. The profiles are normalized to their maximum value.

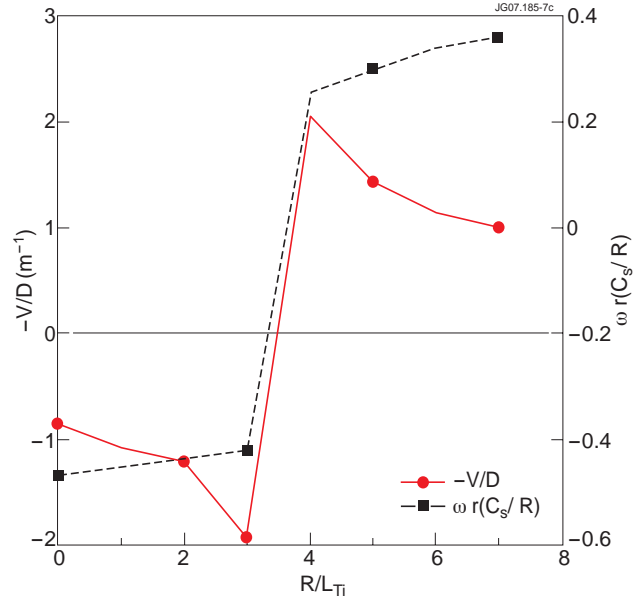


Figure 7: Peaking factors and real frequency (normalized to the sound speed and to the major radius) predicted by GS2 for Ni in Pulse No: 68383 at $\rho=0.35$ (with a scan on R/L_{Ti}).